

Feasibility and Performance Analysis of Cylinder Deactivation for a Heavy-Duty Compressed Natural Gas Engine

*Original*

Feasibility and Performance Analysis of Cylinder Deactivation for a Heavy-Duty Compressed Natural Gas Engine / Misul, DANIELA ANNA; Scopelliti, Alex; Di Maio, Dario; Napolitano, Pierpaolo; Beatrice, Carlo. - In: ENERGIES. - ISSN 1996-1073. - ELETTRONICO. - 17:(2024). [10.3390/en17030627]

*Availability:*

This version is available at: 11583/2985442 since: 2024-02-21T14:27:07Z

*Publisher:*

MDPI

*Published*

DOI:10.3390/en17030627

*Terms of use:*

This article is made available under terms and conditions as specified in the corresponding bibliographic description in the repository

*Publisher copyright*

(Article begins on next page)

## Article

# Feasibility and Performance Analysis of Cylinder Deactivation for a Heavy-Duty Compressed Natural Gas Engine

Daniela Anna Misul <sup>1,\*</sup>, Alex Scopelliti <sup>1</sup>, Dario Di Maio <sup>2</sup>, Pierpaolo Napolitano <sup>2</sup> and Carlo Beatrice <sup>2</sup>

<sup>1</sup> Dipartimento Energia, Politecnico di Torino, 10129 Torino, Italy; alex.scopelliti@polito.it

<sup>2</sup> Consiglio Nazionale delle Ricerche—Istituto di Scienze e Tecnologie per l'Energia e la Mobilità Sostenibili, 80125 Naples, Italy; dario.dimaio@stems.cnr.it (D.D.M.); pierpaolo.napolitano@stems.cnr.it (P.N.); carlo.beatrice@stems.cnr.it (C.B.)

\* Correspondence: daniela.misul@polito.it

**Abstract:** The rising interest in the use of gaseous fuels, such as bio-methane and hydro-methane, in Heavy-Duty (HD) engines to reduce Greenhouse Gases pushed by the net-zero CO<sub>2</sub> emissions roadmap, introduced the need for appropriate strategies in terms of fuel economy and emissions reduction. The present work hence aims at analysing the potential benefits derived from the application of the cylinder deactivation strategy on a six-cylinder HD Natural Gas Spark Ignition (SI) engine, typically employed in buses and trucks. The activity stems from an extensive experimental characterisation of the engine, which allowed for validating a related 1D model at several Steady-State conditions over the entire engine workplan and during dynamic phases, represented by the World Harmonized Transient Cycle (WHTC) homologation cycle. The validated model was exploited to assess the feasibility of the considered strategy, with specific attention to the engine working areas at partial load and monitoring the main performance parameters. Moreover, the introduction in the model of an additional pipeline and of valves actuated by a dedicated control logic, allowed for embedding the capability of using Exhaust Gas Recirculation (EGR). In the identified operating zones, the EGR strategy has shown significant benefits in terms of fuel consumption, with a reduction of up to 10%. Simultaneously, an appreciable increase in the exhaust gas temperature was detected, which may eventually contribute to enhance the Three-Way Catalyst (TWC) conversion efficiency. Considering that few efforts are to be found in the literature but for the application of the cylinder deactivation strategy to Light-Duty or conventionally fuelled vehicles, the present work lays the foundation for a possible application of such technology in Natural Gas Heavy-Duty engines, providing important insights to maximise the efficiency of the entire system.

**Keywords:** cylinder deactivation; modelling; biogas engine; emissions; thermal efficiency



**Citation:** Misul, D.A.; Scopelliti, A.; Di Maio, D.; Napolitano, P.; Beatrice, C. Feasibility and Performance Analysis of Cylinder Deactivation for a Heavy-Duty Compressed Natural Gas Engine. *Energies* **2024**, *17*, 627. <https://doi.org/10.3390/en17030627>

Academic Editors: Georgios Mavropoulos, E.C. Andritsakos and Roussos G. Papagiannakis

Received: 19 December 2023

Revised: 19 January 2024

Accepted: 25 January 2024

Published: 28 January 2024



**Copyright:** © 2024 by the authors. Licensee MDPI, Basel, Switzerland. This article is an open access article distributed under the terms and conditions of the Creative Commons Attribution (CC BY) license (<https://creativecommons.org/licenses/by/4.0/>).

## 1. Introduction

In recent years, a lot of research and development has been carried out to improve internal combustion engines efficiency to reduce Greenhouse Gases (GHGs) and air pollutant emissions in order to meet the increasingly stringent regulations. These new emissions standards come from the higher concern and visible changes in global warming and people's health. In fact, unregulated GHGs will lead to increasing warming, with the estimation of reaching 1.5 °C above the 1850–1900 reference, in the near term in the modelled scenarios [1], whereas air pollution is the single largest environmental health risk in Europe [2]. Since the transportation sector is the second-largest source of energy-related CO<sub>2</sub> emissions globally, contributing 25% of the total energy-related CO<sub>2</sub> emissions [3], new studies and new technologies are becoming more and more relevant to preserve the safety of the people and the world in a view of sustainable development. In this perspective, alternative fuels are useful, especially in the Heavy-Duty sector, to decrease the content of net carbon dioxide and pollutants emitted in the environment by exploiting their composition and production [4].

Engines powered by gaseous fuels, as the one analysed in this study, represent an important step in short term towards the net-zero greenhouse gas emissions EU targets, thanks to the lower CO<sub>2</sub> emitted and the increase in thermal efficiency, which can reach values up to +10% [5]. In particular, biogas composed mainly of Methane (CH<sub>4</sub>) and Compressed Natural Gas (CNG) mixtures appears highly promising for reducing carbon emissions. At the same time, new technologies, such as Cylinder Deactivation (CDA), can be useful to directly reduce the fuel consumption and CO<sub>2</sub> and pollutants emissions [6,7]; the latter can also be employed to increase the in-cylinder temperatures, ensuring increased catalyst conversion efficiency [8]. The combination of these solutions is very interesting, especially in HD applications, where further development is possible. In addition, the activity could be even extended to innovative propulsion systems run by zero or near-zero carbon emissions fuels such as hydrogen to combine their benefits [9].

Among the successful improvements, CDA has started to have more and more importance, due to its capability of reducing fuel consumption [6,7]. The benefits are achieved in part-load operations where, by deactivating some cylinders, the load on the active cylinders increases, allowing to work at higher efficiency and thus lower Brake Specific Fuel Consumption (BSFC) [6]. The main advantages of the cylinder deactivation strategy are summarised in the following.

- Higher efficiency: the benefit is higher for larger engines because they work at lower loads, and for low engine speed and low gears due to higher throttling at low gears [10].
- Lower pumping losses in SI engine: the throttling device can be maintained open wider due to the increased requested load [6,10,11].
- Improved combustion and lower cylinder-wall heat losses [12].
- Lower emissions: the catalyst conversion efficiency is increased due to higher temperature at the exhaust [6,13].

Nevertheless, this strategy has some drawbacks that are similarly reported.

- Frictional losses increase: the increase in working cylinders is not compensated by the decrease in deactivated cylinders, especially at connecting rod, piston rings and bearings [6,14].
- Mixed lubrication and increased engine oil consumption: the former is caused by higher temperature and pressure on the bearings. In this case, the use of special coatings and a precise minimum lubricant film thickness can solve the problem. This kind of lubrication can lead to significant power losses [15]. The latter is caused by lower in-cylinder pressure during the intake stroke and lower temperature of the piston rings in the deactivated cylinders. The increased introduction of oil due to more frequent movements of the top ring can also cause higher exhaust smoke. In these cases, solutions can be reducing the ring grooves clearances or ring gap dimensions [6,16]. In addition, uneven and increased wear can arise due to the reduced lubricant film thickness and pressure peaks inside the cylinder [6,14].
- Noise Vibration Harshness (NVH) characteristics: the changes in pressure pulses and reduction in firing frequency causes greater torsional forces and speed fluctuations. The effect can be mitigated by employing a dual-mass flywheel or a centrifugal pendulum adsorber [6,17].
- Compressor surge line: deactivating some cylinders can result in a movement of the surge line to the right, with a consequent greater sensitivity to the pulsations frequency [18].
- Higher temperature on components: especially in the upper section of the cylinders liners and the lower part of the exhaust valves [19].
- Increased gas leakage: these losses are however overcome by the CDA benefits [6].

Cylinder deactivation can be classified according to the charge trapped in the inactive cylinders:

- Exhaust gas: this leads to higher temperatures which, in turn, cause greater crankshaft irregularities, higher friction, and work loss due to the blow-by. Thus, the deactivation must be maintained for at least 10 cycles to achieve a stabilisation of the pressure and the fuel consumption benefit. However, the cylinders cool down more slowly, so they are reactivated more easily [20].
- Fresh air: it gives lower pressures and irregularities on the crankshaft but has issues when reactivating the cylinder due to the loss of tumble or swirl. Introducing fresh charge could also cause unnecessary enrichment caused by the oxygen sensor detecting fresh air [6].
- Empty cylinder: avoiding opening the intake valves after the exhaust gases are expelled, the cylinder remains in an almost vacuum state. This can lead to very important benefits, but has the considerable drawback of oil suction into the combustion chamber [6].

The number of deactivated cylinders can be fixed in the so-called selective or fixed CDA, having some predetermined cylinders that deactivate. Another option is the rolling CDA, in which each of the cylinders can be deactivated at any time, giving the possibility to change the number of active cylinders from cycle to cycle. This technology has the advantage of further reducing the fuel consumption and the possibility of bypassing the firing frequencies that would generate high levels of vibration. It also prevents uneven wear and oil suction into the chamber, given that each cylinder is deactivated for a shorter time. An example of the rolling method is the Dynamic Skip Fire (DSF), an advanced control strategy that makes deactivation decisions for every cylinder on an individual firing opportunity basis [6,21].

The transition to the deactivation mode must be quick to guarantee a responsive engine: the Engine Control Unit (ECU) controls the throttle, the ignition timing and the injection to prevent variations in the torque, and does so when some prescribed conditions are achieved, e.g., engine speed and temperature, torque, and catalytic converter temperature. For this category of engines, in fact, the aspect of gaseous fuel injection plays a major role [22], which should be properly conceived in case of CDA. The goal is to maintain the same torque before and after the deactivation: it is usually performed by adjusting the valve overlap, the manifold pressure, and/or retarding the ignition timing in relation to the charge volume [6,12].

Cylinder deactivation can be implemented in several ways: the simplest way would be to deactivate the fuel injection, without applying valve proper deactivation. In this case; however, the consumption benefit is quite low, pumping losses are not reduced and drops in the exhaust gases temperature are expected [6]. CDA and its valve deactivation systems can be subdivided into hydraulically and electro-mechanically controlled systems. The former include technologies such as: switchable roller finger follower [23], hydraulic valve tappets [24], and switchable pivot element with a hydraulic lash adjuster [25]. Electro-mechanically controlled systems have slower responses but are simpler than hydraulic ones. They include: electro-mechanical roller follower [26], switchable rocker arm [6], movable cam sections [12], engine with skip cycle mechanism [17], and Variable Valve Actuation (VVA) [20,27].

Internal Exhaust Gas Recirculation (iEGR) can be exploited when cylinder deactivation systems are installed only on the inlet side, thus reducing the economical effort to change the hardware. An example is reported in [28], where an effective combination of cylinder deactivation with a MultiAir VVA leads to minimising the pumping losses, being effective in the low load and low speed region.

The modelling activity performed in the present study has been carried out initially to verify the feasibility of CDA, simulating a fixed cylinder deactivation with the presence of a valve deactivation mechanism. Subsequently, a method that excludes the valve deactivation in the CDA strategy has been analysed, requiring less hardware modification. The latter has been performed with the employment of Exhaust Gas Recirculation (EGR), exploiting the addition of a pipe connecting the exhaust manifold of one branch of the engine to the intake

one. The possible benefits and criticalities have been analysed, with specific reference to the target torque, to the fuel consumption reduction, and to the exhaust temperature increase.

## 2. Model and Experimental Campaign

This section aims to describe the engine model and the methodology adopted to choose the suitable cylinder deactivation configuration to achieve a reasonable trade-off in terms of additional hardware, costs, and benefits.

### 2.1. Engine Model Description

The study has been performed on the 1D model of a six-cylinder heavy-duty engine, whose characteristics are reported in Table 1.

**Table 1.** Engine specifications.

Engine Specifications	Values
Type	Turbocharged, CNG, SI
Cylinders arrangement	6 cylinders in line
Engine displacement	12.9 L
Bore	135 mm
Stroke	150 mm
Compression ratio	12:1
Rated power	338 kW @ 2000 rpm
Torque	2000 Nm @ 1100–1620 rpm
Valves per cylinder	4
Injection system	Multi-Point Injection (MPI)
Air-fuel equivalence ratio $\lambda$	1
Turbocharger control	Wastegate valve
After-treatment system	Three-Way Catalyst

The six-cylinder engine model is characterised by a semi-predictive combustion sub-model, which had been calibrated, in previous works [29], through a Three-Pressure Analysis approach for each specific operating condition in the engine workplan with a defined burn rate, following a well-established calibration procedure [30,31]. Hence, the original model has been run to create a baseline set of results to evaluate the benefits of the CDA solutions.

The geometry, material properties, and all the specifications of the standard six-cylinder configuration were already included in the original model [29].

### 2.2. Steady-State Model Feasibility Study

The first part of the work aims at analysing all possible deactivation configurations, in terms of torque output and hardware complexity, as well as of obtained benefits and criticalities. A steady-state simulation has hence been performed, exploiting 25 operating conditions on the engine map at different speeds and loads, for which data had been collected from experiments. The considered engine working points are reported in Figure 1.

Several performance parameters have been considered for the validation of the engine model in Steady-State in the different operating conditions of the entire workplan, including heat exchanges and combustion submodel.

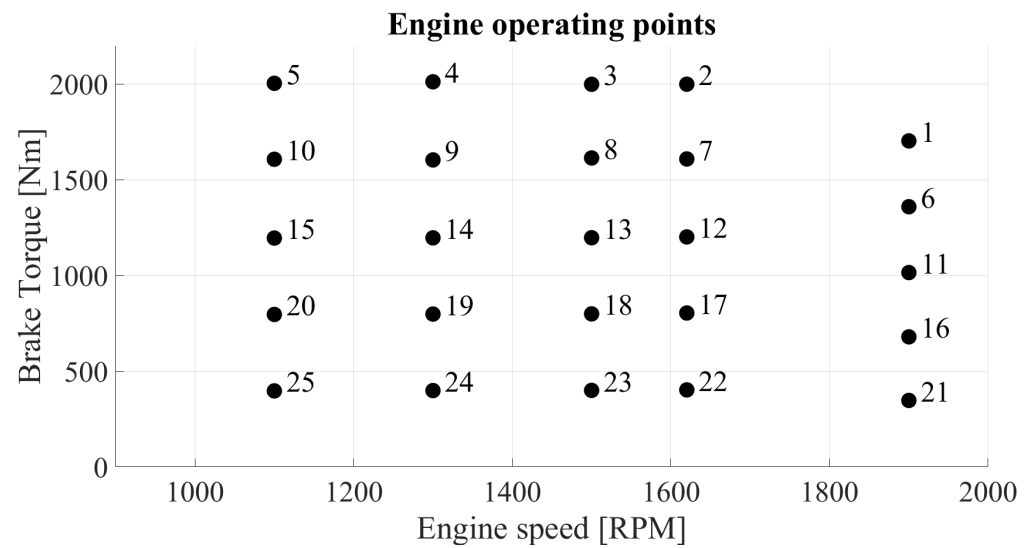


**Figure 1.** The 25 selected engine operating points in the workplan.

As a following step, a model with fixed cylinders deactivation has been analysed, considering the engine working with either 3, 4, or 5 active cylinders. This has been performed by deactivating the fuel injection in the manifolds of the inactive cylinders (removing the injectors in the 1D model) and by impairing the intake and exhaust valves lift. A virtual controller actuates the throttle valve, changing its opening based on the required torque target. At the same time, the Air-to-Fuel Ratio is fixed in the injector model. Therefore, the intake air mass flow rate and fuel mass flow rate are defined respecting these conditions.

In the three-cylinder configuration, cylinders 4, 5, and 6 are the ones deactivated. The entire left part on the manifold is therefore deactivated, as is evident from the 'missing' injectors in Figure 2.

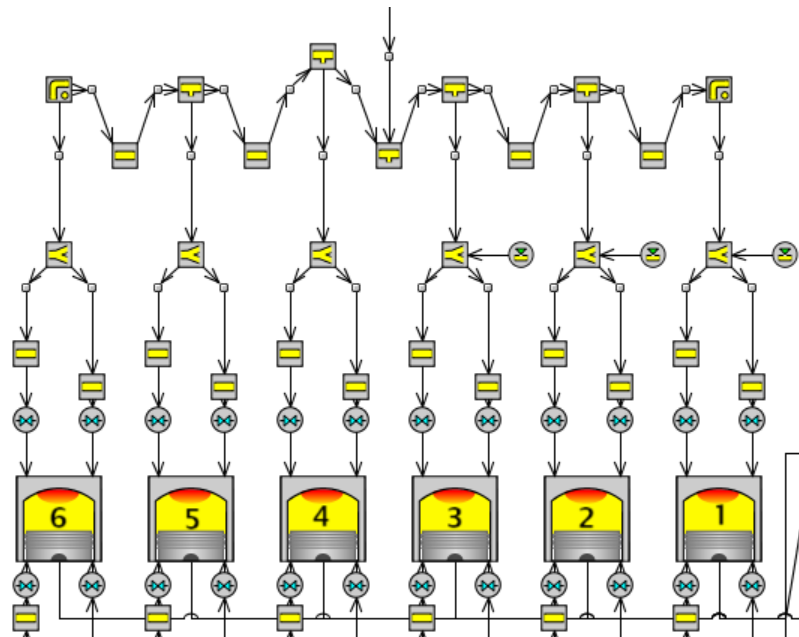


**Figure 2.** Three-cylinder CDA configuration.

Such a choice was selected to guarantee the possibility of having a split between the two separate branches of the manifolds serving the active and the deactivated cylinders.

The four-cylinder configuration deactivates cylinders 2 and 5, whereas the five-cylinder one deactivates cylinder 5.

As for the baseline engine model, each cylinder deactivation configuration has been run in the steady-state simulation throughout the 25 experimental engine operating points, represented in Figure 1. At first, the model allowed for checking on the imposed target brake torque. Predictably, a lower number of active cylinders leads to the impossibility of reaching the highest torque values. However, it should be noted that no control actions have been performed to increase the load. As a matter of fact, the turbocharger could be controlled to provide higher boost pressures, allowing for the achievement of the target torque. Additionally, all configurations share the same original combustion model. Thus, there is room for an even better agreement on the torque value and guarantee the effectiveness of the deactivation strategy if acting on the combustion process, with changes, by way of example, on spark timing and/or the Mass Burned Fraction at 50% (MFB50). Torque differences with respect to the starting six-cylinder engine configuration are reported in Table 2. For each configuration, the operating points leading to percentage values lower than 10% have been considered and are correspondingly highlighted in green.

For each engine configuration, the increase in Brake Thermal Efficiency (BTE) have been calculated as the difference from the six-cylinder engine BTE. Accordingly, three-cylinders shows an average BTE increase of 1.3%, considering the working points at 20% load. A four-cylinder engine reaches +0.9% BTE at 20% and 40% load, whereas five-cylinders shows a BTE increment of 0.7%, at 20, 40, and 60% load cases.

**Table 2.** Torque difference comparison of the three CDA configurations with respect to the baseline 6-cylinder engine.

Case	Torque %	3-Cylinders Torque Difference	4-Cylinders Torque Difference	5-Cylinders Torque Difference
11	60%	−49%	−22%	0%
16	40%	−36%	−7%	0%
21	20%	−7%	−2%	0%
12	60%	−50%	−27%	−5%
17	40%	−37%	−7%	0%
22	20%	−8%	−2%	0%
13	60%	−49%	−27%	−5%
18	40%	−36%	−7%	0%
23	20%	−5%	−2%	0%
14	60%	−48%	−27%	−5%
19	40%	−38%	−10%	0%
24	20%	−6%	−2%	0%
15	60%	−48%	−27%	−6%
20	40%	−40%	−14%	0%
25	20%	−3%	−2%	0%

As reported in Figure 3, considering the three-cylinder configuration, the cases for which the configuration is attainable are the ones with the lowest target torque, corresponding to the 20% of the maximum engine torque. On the other hand, the four-cylinder configuration is effective for the cases in which the torque sums up to the 40% of the engine load (with the sole exception of case 20, which exceeds the 10% gradient), whereas the five-cylinder engine can work up to 60%.

One possible benefit of cylinder deactivation is the increase in exhaust gas temperature, enhancing After-Treatment System (ATS) performances, constituted by the TWC [29]. The enhancement of TWC performance is caused by the reduced light-off delay and by the increase in conversion efficiency, especially in the first phases of transient cycles. To analyse the benefit, temperature values detected at the turbine outlet are proposed (green circle in Figure 4).



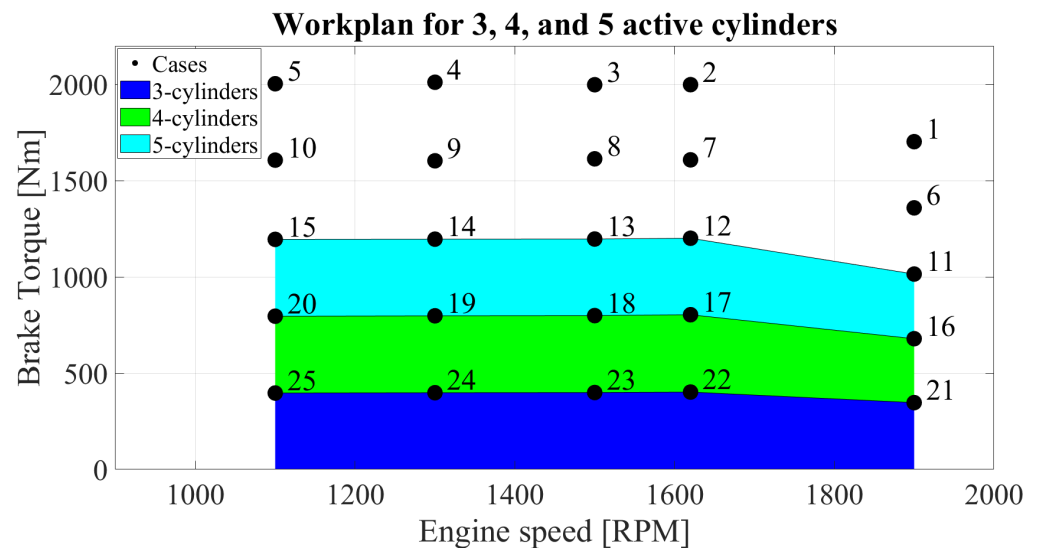


**Figure 3.** Workplan for three, four, and five active cylinders.

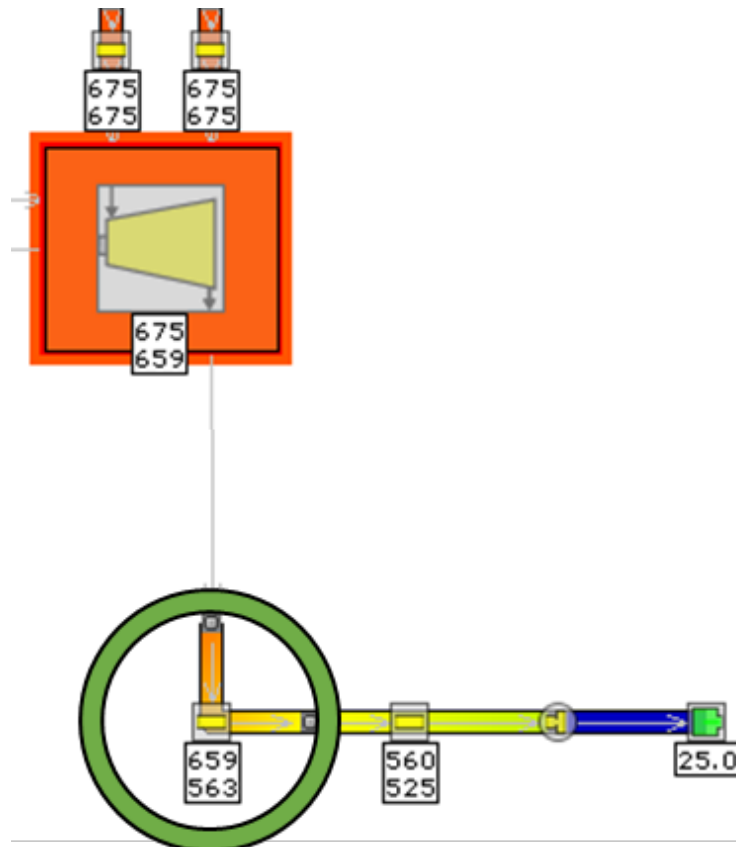


**Figure 4.** Temperature measurement point: the box reports inlet and outlet temperatures of the represented pipe.

The comparison of the temperatures between the original engine and the three CDA configurations in the correspondingly feasible cases is shown in Figure 5.

The three-cylinder results hold for an increase in gas temperatures. Table 3 sums up the previous results for the three-cylinder CDA, highlighting temperatures rises from 38 to 42 °C, corresponding to an increase of about 6%.



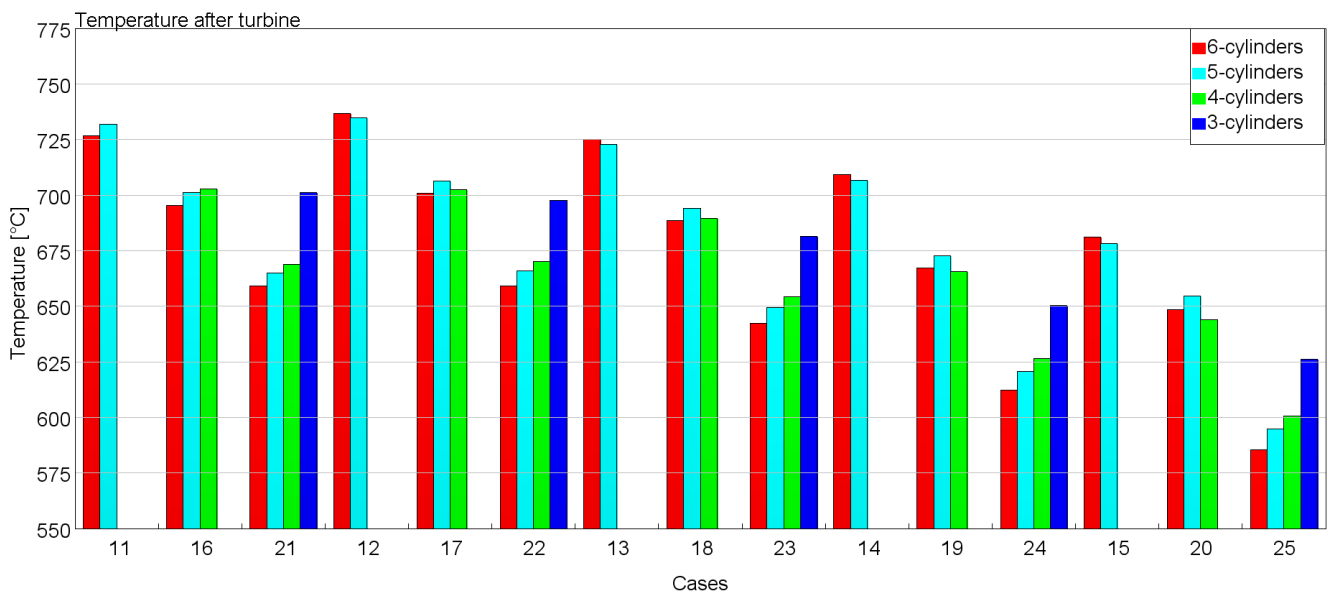


**Figure 5.** Temperature comparison for the three CDA configurations.

**Table 3.** Temperature difference—three-cylinder configuration.

Case	Torque & Engine Speed	6-Cylinders T [°C]	3-Cylinders T [°C]	T Increment [°C]	T Increment [%]
21	20% torque 1900 RPM	659	701	42	6%
22	20% torque 1620 RPM	659	698	38	6%
23	20% torque 1500 RPM	642	682	39	6%
24	20% torque 1300 RPM	612	650	38	6%
25	20% torque 1100 RPM	585	626	41	7%

As far as the two other configurations are concerned, temperature values do not exhibit considerable benefits, partly related to the imperfect reproduction of the required Indicated Mean Effective Pressure (IMEP) due to the use of a fixed combustion submodel, as described above. The four-cylinder configuration holds for an average temperature increment of 6.6%, whereas the five-cylinder one holds up to 3.4%.

The second advantage of cylinder deactivation is fuel consumption reduction. In fact, the cylinders that remain active must work at a higher load with a subsequent shift to a working point with increased thermal efficiency. In addition, the throttle must open wider to allow for a higher air introduction into the active cylinders, thus reducing the pumping losses. This also causes a better charge flow into the cylinders, as made explicit by the volumetric efficiency increase. Table 4 shows the volumetric efficiency increment, evaluated for cylinder n°1, for the three-cylinder configuration with respect to the six-cylinder engine in the five feasible cases. It is worth mentioning that the volumetric efficiency has been measured taking as input the boost pressure and not the atmospheric one, to allow for a clearer understanding of the filling efficiency of the cylinders, thus excluding the influence of the turbocharger.

**Table 4.** Volumetric efficiency increment—three-cylinder configuration.

Case	Torque & Engine Speed	6-Cylinders Volumetric Efficiency [-]	3-Cylinders Volumetric Efficiency [-]	Volumetric Efficiency Increment
21	20% torque 1900 RPM	0.37	0.68	86%
22	20% torque 1620 RPM	0.40	0.73	82%
23	20% torque 1500 RPM	0.40	0.75	85%
24	20% torque 1300 RPM	0.41	0.75	83%
25	20% torque 1100 RPM	0.41	0.77	88%

The volumetric efficiency increment values are much lower for the other two configurations, which reach an average increase of 40% and 14% for the four-cylinder and five-cylinder configuration, respectively. Pumping Mean Effective Pressure (PMEP) would more accurately address such difference (Table 5). PMEP decrements from 70% up to 88% are achieved for the three-cylinder engine, depending on the case considered.

**Table 5.** PMEP decrement—three-cylinder configuration.

Cases	6-Cylinders PMEP [mbar]	3-Cylinders PMEP [mbar]	PMEP Difference [%]
21	−617	−184	−70%
22	−550	−114	−79%
23	−539	−64	−88%
24	−508	−60	−88%
25	−495	−108	−78%

It is also worth considering the change in load for the active cylinders. Figure 6 reports the comparison among the measured Indicated Mean Effective Pressure (IMEP) from cylinder #1. As expected, fewer active cylinders force the active ones to work at higher loads. More specifically, the three-cylinder configuration IMEP is more than doubled in case 21 (9.95 bar versus the experimental 4.76 bar) with respect to the base engine configuration.

The pressure-volume diagram in Figure 7 refers to case 21 and highlights the above-mentioned effects of CDA. The in-cylinder load is increased, and the pumping losses are decreased, thanks to the wider opening of the throttle and to the consequent higher intake pressure. In fact, the lower area, which represents the work exploited to move gas in and out of the cylinder, is smaller for the three-cylinder engine.

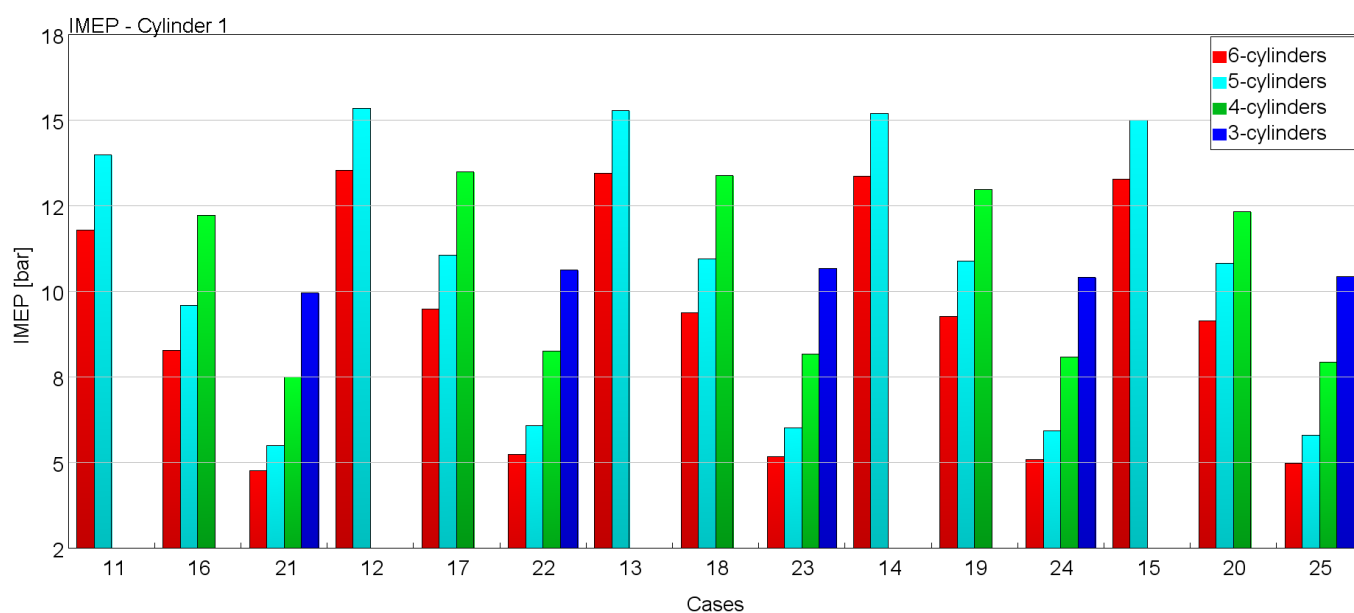


Figure 6. IMEP comparison for the three CDA configurations.

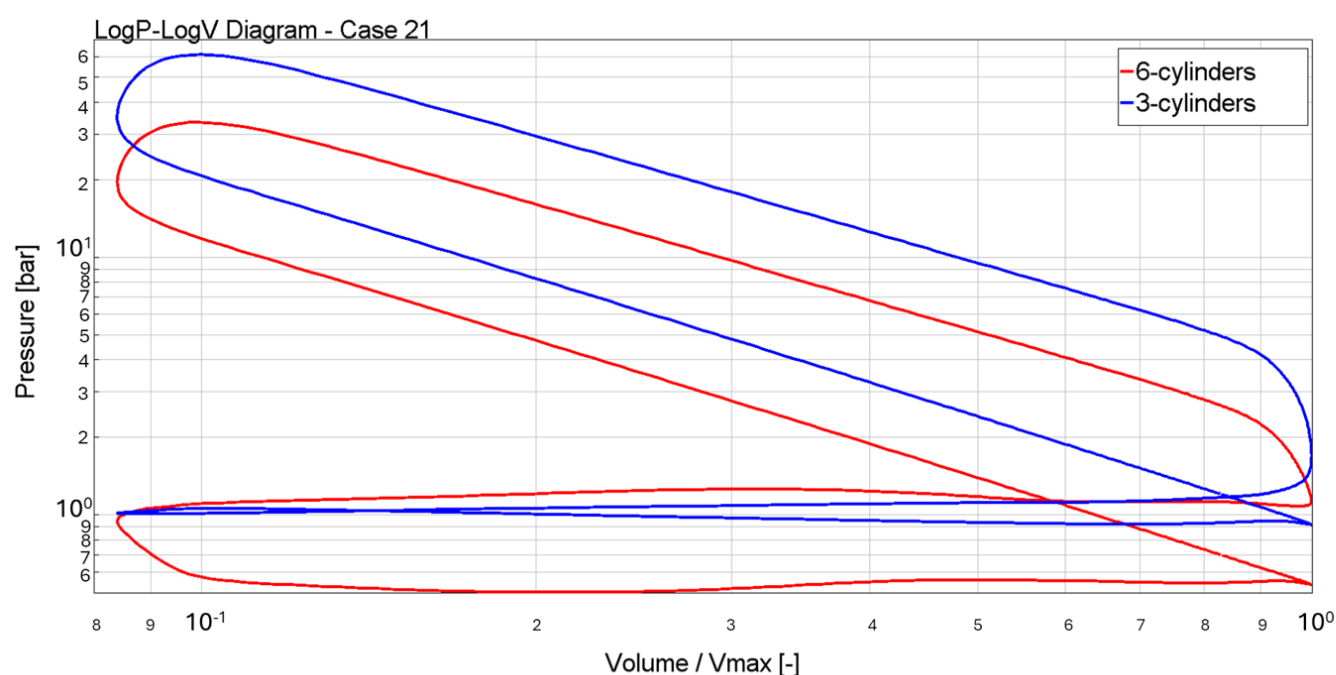


Figure 7. logP-logV diagram—three-cylinder configuration.

The latter results into a fuel consumption benefit: Table 6 shows the fuel flow rate comparisons for each deactivation case. The fuel consumption benefit for the three-cylinder configuration is evident, with reductions up to the 9%. On the other hand, the four-cylinder configuration holds for an average decrease of 7.8%, whereas the five-cylinder one shows a 3.5% decrement.

**Table 6.** Fuel consumption benefit with respect to the starting 6-cylinder configuration.

Cases	3-Cylinders Fuel Flow Rate Decrement	4-Cylinders Fuel Flow Rate Decrement	5-Cylinders Fuel Flow Rate Decrement
11	-	-	−2%
16	-	−10%	−2%
21	−7%	−6%	−3%
12	-	-	−6%
17	-	−8%	−2%
22	−9%	−5%	−3%
13	-	-	−6%
18	-	−9%	−2%
23	−8%	−5%	−3%
14	-	-	−6%
19	-	−11%	−2%
24	−8%	−5%	−3%
15	-	-	−6%
20	-	−14%	−2%
25	−6%	−5%	−3%

### 2.3. Cylinder Deactivation by Exhaust Gas Recirculation

The results of the previous analyses have shown the clear advantages achievable with cylinder deactivation in terms of increased exhaust temperatures and lowered fuel consumption. However, in a real application case, some complications must be considered. For an engine without a VVA system, the considered deactivation solution would require deep hardware modifications to allow for the disablement of the intake and exhaust valves [6].

For this reason, the possibility of acting only on fuel injection and spark timing, without changes on valve lift, has been considered. Nevertheless, fresh air should not be admitted in the deactivated cylinders to avoid releasing it in the exhaust, thus triggering the lambda sensor to inject more fuel. At the same time, the air flow cannot be simply interrupted, or else the deactivated cylinders would run in a quasi-vacuum state which would lead to a oil suction into the chambers. Therefore, a flow must be allowed avoiding fresh air. Given that the engine manifold was basically divided into two main branches, each one serving three cylinders, it was decided to apply a three-cylinder deactivation in one of the branches, exploiting the manifold geometry to drive the gases from the exhaust line of the three cylinders to the upstream of these cylinders themselves.

The three-cylinder configuration has been chosen for its ease of application and for the higher benefits highlighted in the previous analyses. The new design of the engine model is presented in Figure 8. The EGR pipe has been dimensioned to guarantee the connection of the two manifolds. Flow splits with 90° angles have been added to take the gases from the exhaust manifold and to force them to reenter the intake one. A throttle valve has been foreseen and positioned before the EGR intake point (Valve 1). It is, in fact, necessary to isolate the EGR circuit, precluding the introduction of fresh air. Additionally, the valve allows for a pressure drop in the intake, which in turn causes a pressure gradient from the exhaust to the intake manifolds to thrust the gases into the EGR pipe. Valve 1 is closed in correspondence with the cylinder deactivation.

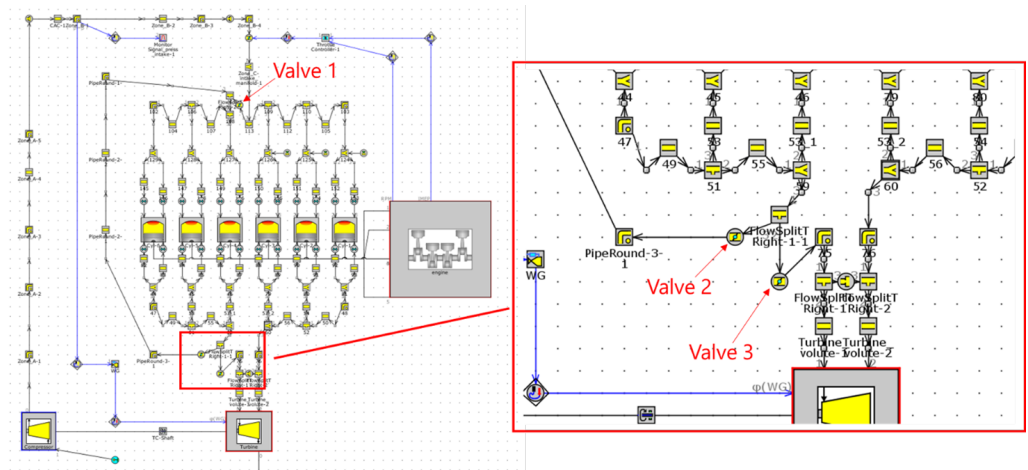


**Figure 8.** EGR pipeline design. Detail of the valves and pipes used in the new 1D engine model.

As a first approximation, all the EGR pipes have been characterised as the exhaust pipes from the original model, including heat transfer model, given the lack of experimental data.

An additional throttle valve (Valve 2) has been added to isolate the circuit during standard functioning (without cylinders deactivation), to avoid fresh mixture to enter the EGR pipe and the exhaust, thus penalising the filling of the cylinders and impairing the engine BMEP.

Valve 3 has been added downstream of the EGR flow split to avoid temperature losses. In fact, given that the left and right manifolds are connected in the proximity of the turbine, during deactivation the hot gases entering the turbine volutes from the right manifold would be mixed with the cooler EGR gases, thus resulting in a lower temperature entering the turbine. Therefore, valve 3 is closed during deactivation to hinder temperature losses.

The steady-state results have been obtained by initialising the simulations to the results of the six-cylinder configuration.

Furthermore, Valve 3 has been kept open at a  $5^\circ$  angle to depressurise the circuit still maintaining a high temperature. A complete closure of the valve would, in fact, produce high gas temperatures, thus inducing high pressure levels in the circuit. The latter would lead to a higher compression work and a consequent loss of BMEP in the deactivated cylinders.

The obtained BMEP is reported in Table 7, with values close to the target full engine ones. It is anyhow worth remembering that the model presents a gap with the target torque. Nevertheless, the decrement is limited, and the target could easily be covered with further model modifications.

**Table 7.** BMEP decrement—EGR configuration.

Case	6-Cylinders BMEP [bar]	3-Cylinders EGR BMEP [bar]	BMEP Difference [%]
21	3.4	3.2	−6%
22	3.9	3.7	−5%
23	3.9	3.9	−1%
24	3.9	3.7	−4%
25	3.9	3.8	−1%

The turbine discharge temperatures analysis returns the expected increments (Table 8), with values up to  $+62^\circ\text{C}$ .

**Table 8.** Temperature increment—EGR configuration.

Case	6-Cylinders T [°C]	3-Cylinders EGR T [°C]	T Increment [°C]	T Increment [%]
21	659	708	49	7%
22	659	708	48	7%
23	642	694	52	8%
24	612	665	53	9%
25	585	648	62	11%

The last analysis concerns the fuel consumption. The results show decrements from 6% to 9% in the five deactivation cases and are reported in Table 9 and compared to the previous model that exploits the valve closure.

**Table 9.** Fuel consumption decrement—EGR configuration.

Case	First, Model Fuel Flow Rate Difference [%]	EGR Fuel Flow Rate Difference [%]
21	−7%	−9%
22	−9%	−8%
23	−8%	−6%
24	−8%	−7%
25	−6%	−6%

Summarising, the definitive engine configuration has given the results reported in Table 10, which are considered satisfactory to proceed with the transient analysis.

**Table 10.** CDA steady-state results—EGR configuration.

Case	BMEP Difference [%]	T Increment [%]	Fuel Flow Rate Difference [%]
21	−6%	7%	−9%
22	−5%	7%	−8%
23	−1%	8%	−6%
24	−4%	9%	−7%
25	−1%	11%	−6%

### 3. Transient Analysis

In the following section, the methodology carried out to analyse cylinder deactivation in transient conditions will be explained. For the sake of brevity, a representative portion of the World Harmonized Transient Cycle (WHTC) was used given the wide range of different conditions, including cut-offs and extended deactivation operations.

Several modifications to the model were needed to achieve the target torque throughout the cycle. The torque measured experimentally is negative during cut-offs because of the dynamometer being attached, so the model would attempt to assign negative values. A dedicated logic control has hence been added to the throttle actuator, with the aim of imposing the experimental air mass flow rate in place of the torque during cut-off operations [29]. Moreover, in the air-controlled phases, the fuel-to-air equivalence ratio  $\phi$  is set equal to zero, so that fuel injection is suppressed, and torque values are comparable to the experimental ones based on the calibrated friction model. A detail of this logic is shown in

Figure 9. The signal generator contains a flags array that makes the controller switch when the imposed torque becomes negative.

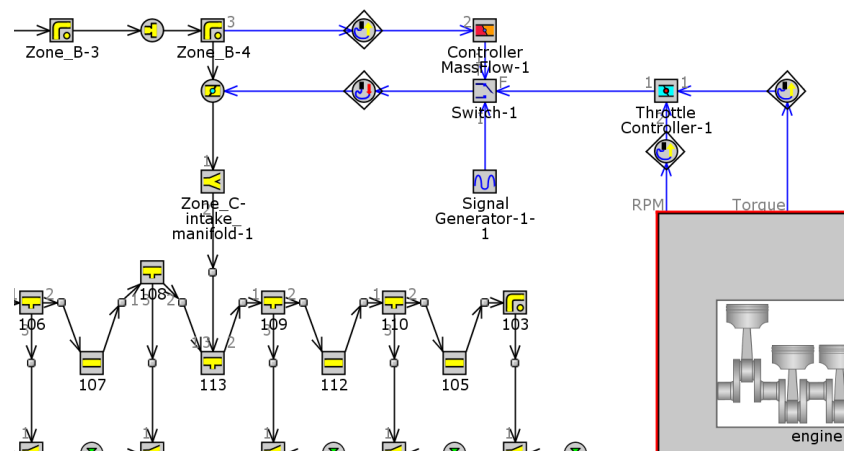


Figure 9. Integration of a control logic in the engine model to reproduce dynamic conditions.

The CDA model with EGR pipe was therefore adapted to the transient cycle to allow for continuous activation and deactivation. For the sake of control simplicity, the three throttle valves used to isolate the EGR circuit have been modelled with the object “OrificeConn”, which can vary its diameter. As in the previously analysed situation, a cylinder deactivation strategy is triggered in conditions with torque lower than 20% of the maximum, i.e., 410 Nm.

Additional modifications have been made to the model avoid thermal losses during the active engine zones, caused by the flow split added in CDA configuration. The latter is needed to drive the exhaust gas and recirculate it into the cylinders (Figure 10).

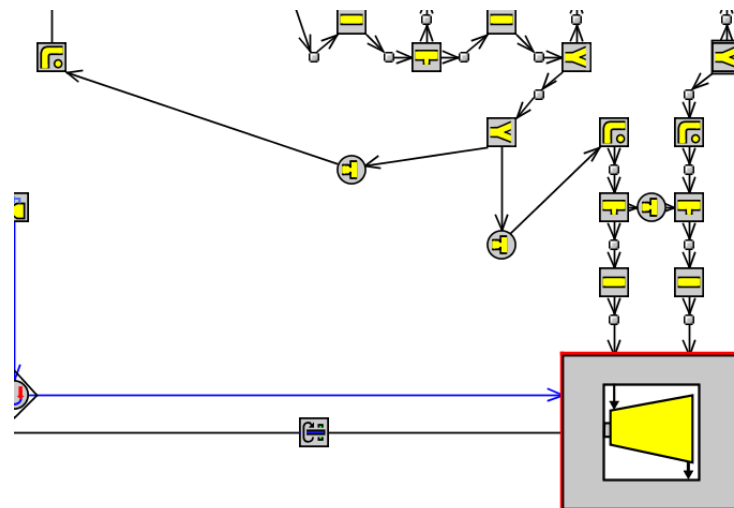


Figure 10. Particular of the flow split added to connect the EGR pipe.

The volume of the flow split has hence been minimised to mitigate the temperature decrease of the exhaust gases.

Some further modifications have been performed to improve the model. The exhaust circuit has been initialised with higher wall temperatures, to simulate the previous part of the WHTC. Furthermore, in order to simplify the management of the flow split, the previous “FlowSplitTRight” object has been replaced with a “FlowSplitGeneral”. The latter in fact gives the possibility to directly choose the volume of the part.

As a final modification, the heat transfer multiplier of the EGR pipes has been changed from the one taken from exhaust pipes to the default value (as the intake pipes are characterised), since the deactivation configuration does not have experimental values.



### Transient Analysis Results

In order to have an overview of the different dynamic conditions, typical of real driving conditions, a portion of the WHTC from 560 s to 670 s has been selected. This choice reflects the need to study short but frequent cut-off periods and longer and more numerous deactivation zones after high torque operations, avoiding a starting condition with very low torque, which would not sufficiently warm up the engine. As a first step, the original engine model has been run to create a comparison baseline set of data. The engine speed and torque have been imposed from experimental data with respect to the WHTC cycle. Additionally, fuel–air equivalence ratios and boost pressures have been taken from the experimental WHTC engine workplan.

Figure 11 shows the torque comparison to the six-cylinder engine model. The starting six-cylinder model reproduces the reference torque of the cycle with a sufficient degree of accuracy. A larger gap is present in the last 10 s of the cycle, due to a numerical instability to be further investigated, in which CDA strategy will not be applied. This leads to the torque deviation shown in Figure 12, which displays a  $R^2$  value of 0.84. The CDA model replicates the baseline results and produces a torque deviation with a  $R^2$  value of about 0.85 (Figure 13). Therefore, they both reproduce the operating conditions with a similar grade of accuracy.

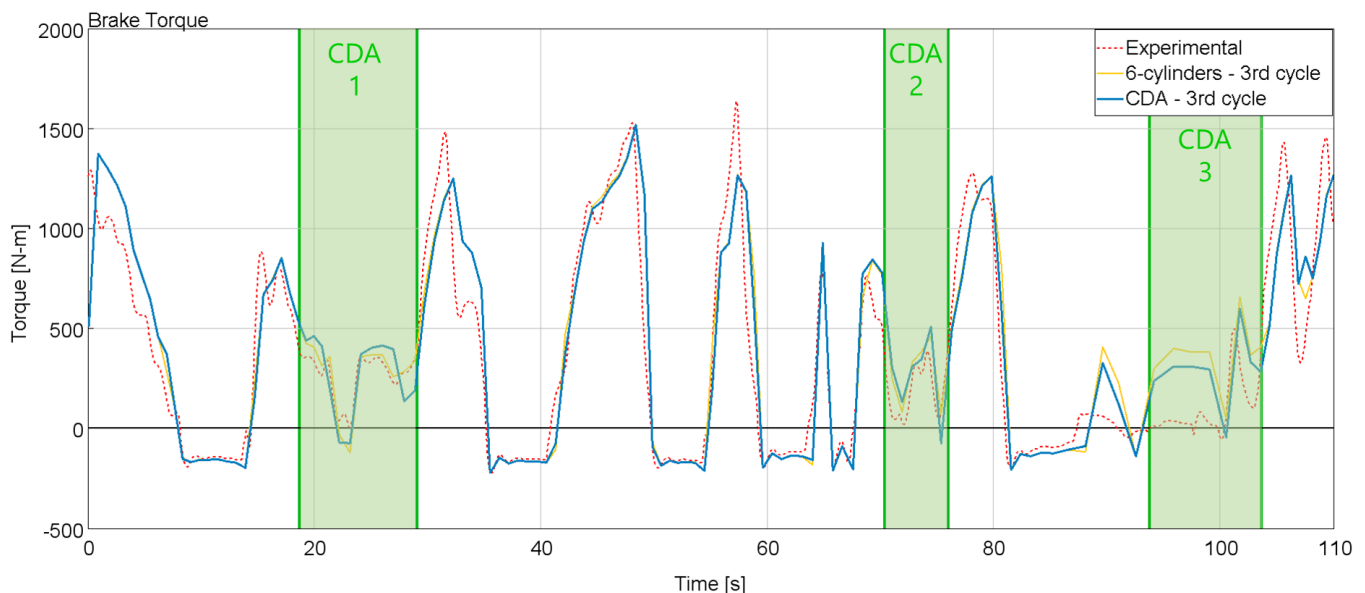


**Figure 11.** Torque comparison—transient cycle.

The cycle turbine-out temperatures are plotted in Figure 14. The small deviations arising in the first 20 s are due to a minimum cycle portion in which CDA occurs, which increases the temperature with respect to the baseline configuration. A decrease appears in the subsequent cut-off (around 10 s), caused by the sudden opening of the deactivated manifold, which is cooler than the active one. Subsequently, the CDA temperature values are almost equal to the six-cylinder ones until the timeframe called “CDA 1” is reached. In “CDA 1” zone, the increment is evident and leads to a rise ranging around +42 °C. Still, when the engine goes back to the activation mode, the CDA plot shows lower temperatures in all active zones and cut-off operations. The other two considered deactivation zones show a maximum increment of +29 °C and +19 °C, respectively. The average temperatures of the three analysed zones are reported in Table 11.

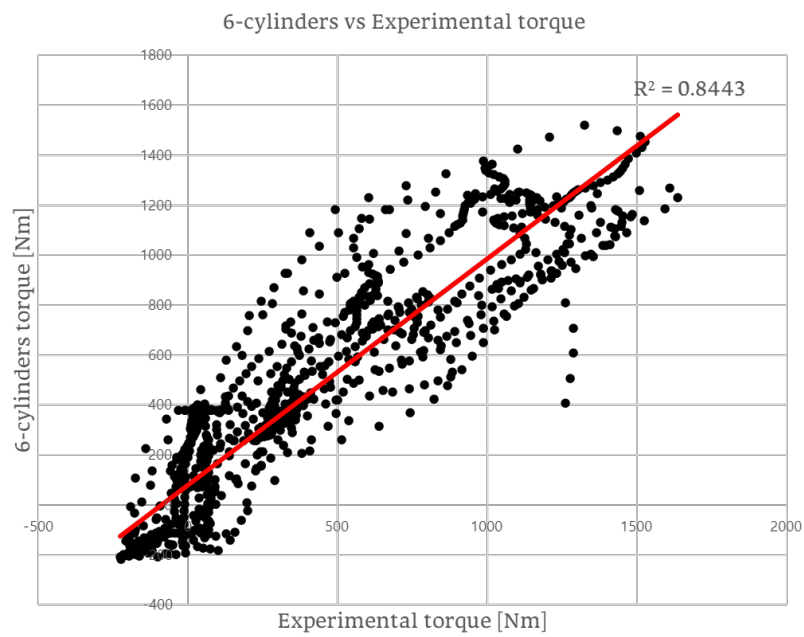


Figure 12. Torque deviation—six-cylinder model vs. experimental.

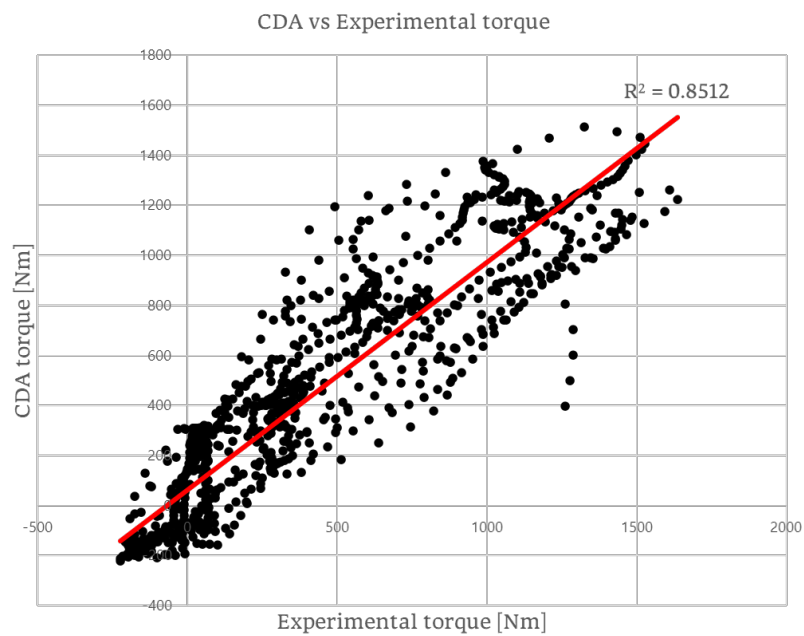
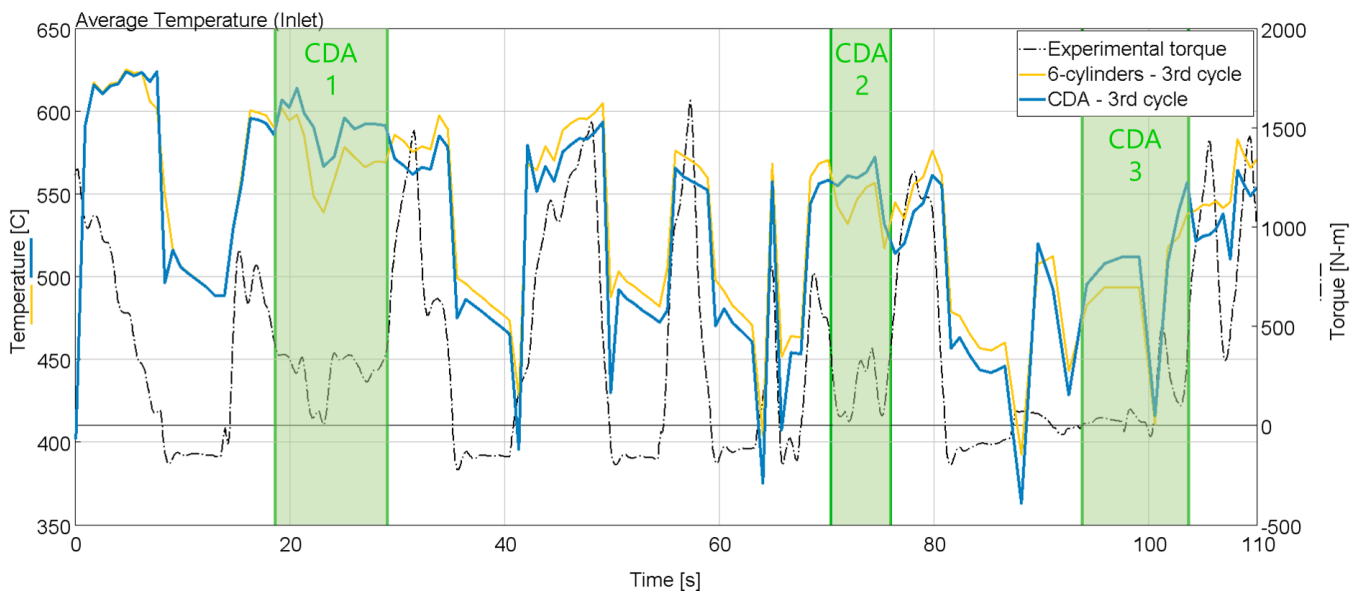


Figure 13. Torque deviation—CDA model vs. experimental.

Table 11. Average temperature increment—transient cycle.

Transient Cycle					
CDA 1		CDA 2		CDA 3	
Average T Difference [°C]	Average T Difference	Average T Difference [°C]	Average T Difference	Average T Difference [°C]	Average T Difference
+19	+3%	+16	+3%	+12	+2%



**Figure 14.** Temperature comparison—transient cycle.

Moving to fuel consumption, the fuel mass flow rate plot is reported in Figure 15. Fuel consumption is consistent with the six-cylinder simulation one and the decrements are appreciable in the CDA zones, especially in the “CDA 3”, where it reaches a value of  $-26\%$ . It is anyhow worth observing that such high benefit might be caused by the fact that six-cylinder model goes to higher than necessary torque values. The average fuel benefit for each of the three zones is reported in Table 12.

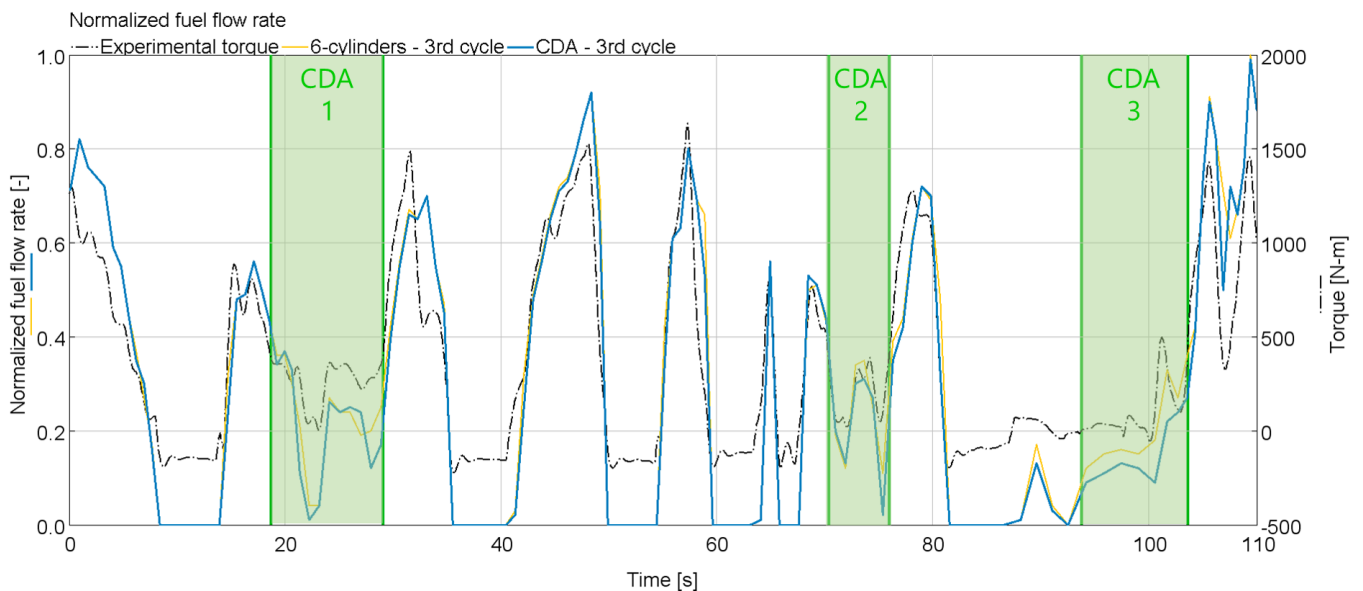


**Figure 15.** Fuel flow rate comparison—transient cycle.

Finally, the overall fuel benefit, excluding “CDA 3” zone, is  $-3.4\%$ .

**Table 12.** Average fuel flow rate decrement—transient cycle.

Transient Cycle					
CDA 1		CDA 2		CDA 3	
Average Fuel Flow Rate Difference [kg/h]	Average Fuel Flow Rate Difference	Average Fuel Flow Rate Difference [kg/h]	Average Fuel Flow Rate Difference	Average Fuel Flow Rate Difference [kg/h]	Average Fuel Flow Rate Difference
−0.9	−8%	−1.1	−10%	−2.7	−26%

#### 4. Conclusions

In this work, different cylinder deactivation analysis strategies were proposed for a six-cylinder HD engine fuelled with CNG. The main conclusions can be summarized as follows:

- Among the several configurations proposed, the fixed three-cylinder deactivation, by recirculating exhaust gas in the three deactivated cylinders, can be considered as the most promising one, thanks to the high benefit in fuel consumption and exhaust gases temperature with temperature increases up to 62 °C in the SS operating tested condition at 20% torque, and up to 19 °C during the selected WHTC portion considered, in which the major fuel reduction benefits are present (up to −10%).
- This study sets the stage for an application of a cylinder deactivation strategy also in large displacement heavy-duty engines, which is currently only implemented in some passenger cars, with the utilisation of simple hardware modifications. The exhaust temperature increment can enhance the Three-Way Catalyst (TWC) performances in terms of conversion efficiency in standard operating conditions, allowing to speed up the reach of the light-off temperature, encouraging a potential reduction in the amount of noble materials or the volume of the catalytic converter.
- An extensive experimental characterisation will be carried out as one of the future developments of the activity, in order to validate the concept and promote a deeper understanding of the working areas in which CDA strategy can be adopted.

**Author Contributions:** Conceptualization, D.D.M., D.A.M. and C.B.; methodology, D.D.M.; software, A.S. and D.D.M.; validation, D.D.M.; formal analysis, D.D.M. and D.A.M.; investigation, A.S. and D.D.M.; data curation, D.D.M. and A.S.; writing—original draft preparation, A.S. and D.D.M.; writing—review and editing, D.D.M., D.A.M. and P.N.; visualization, A.S. and D.D.M.; supervision, D.A.M., C.B. and P.N. All authors have read and agreed to the published version of the manuscript.

**Funding:** This research received no external funding.

**Data Availability Statement:** The data presented in this study are available on request from the corresponding author.

**Conflicts of Interest:** The authors declare no conflicts of interest.

#### Abbreviations

ATS	After-Treatment System
BSFC	Brake Specific Fuel Consumption
BTE	Brake Thermal Efficiency
CDA	Cylinder Deactivation
CNG	Compressed Natural Gas
DSF	Dynamic Skip Fire
ECU	Engine Control Unit
EGR	Exhaust Gas Recirculation
GHGs	Greenhouse Gases
HD	Heavy-Duty
iEGR	Internal Exhaust Gas Recirculation

IMEP	Indicated Mean Effective Pressure
MFB50	Mass Burned Fraction at 50%
NVH	Noise Vibration Harshness
PMEP	Pumping Mean Effective Pressure
SI	Spark Ignition
TWC	Three-Way Catalyst
VVA	Variable Valve Actuation
WHTC	World Harmonized Transient Cycle

#### Glossary

$\lambda$	Air–fuel equivalence ratio
$\phi$	Fuel–air equivalence ratio
CO <sub>2</sub>	Carbon dioxide

## References

1. Intergovernmental Panel on Climate Change IPCC. *Synthesis Report of the IPCC Sixth Assessment Report (AR6)*; Technical Report; IPCC: Geneva, Switzerland, 2023.
2. European Environment Agency. *The European Environment: State and Outlook 2020: Knowledge for Transition to a Sustainable Europe*; Publications Office of the European Union: Luxembourg, 2019; 496p.
3. United Nations Environment Programme. *Emissions Gap Report 2022, The Closing Window, Climate Crisis Calls for Rapid Transformation of Societies*; UNEP: Nairobi, Kenya, 2022.
4. IEA. *World Energy Outlook 2022*; IEA: Paris, France, 2022. Available online: <https://www.iea.org/reports/world-energy-outlook-2022> (accessed on 19 December 2023).
5. Khan, M.I.; Yasmin, T.; Shakoor, A. Technical overview of compressed natural gas (CNG) as a transportation fuel. *Renew. Sustain. Energy Rev.* **2015**, *51*, 785–797. [\[CrossRef\]](#)
6. Fridrichová, K.; Drápal, L.; Vopařil, J.; Dluhoš, J. Overview of the potential and limitations of cylinder deactivation. *Renew. Sustain. Energy Rev.* **2021**, *146*. [\[CrossRef\]](#)
7. Zhao, J.; Xi, Q.; Wang, S.; Wang, S. Improving the partial-load fuel economy of 4-cylinder SI engines by combining variable valve timing and cylinder-deactivation through double intake manifolds. *Appl. Therm. Eng.* **2018**, *141*, 245–256. [\[CrossRef\]](#)
8. Douglas, K.J.; Milovanovic, N.; Turner, J.W.G.; Blundell, D. *Fuel Economy Improvement Using Combined CAI and Cylinder Deactivation (CDA)-An Initial Study*; SAE International: Warrendale, PA, USA, 2005.
9. Sun, Z.; Hong, J.; Zhang, T.; Sun, B.; Yang, B.; Lu, L.; Li, L.; Wu, K. Hydrogen engine operation strategies: Recent progress, industrialization challenges, and perspectives. *Int. J. Hydrogen Energy* **2023**, *48*, 366–392. [\[CrossRef\]](#)
10. Leone, T.G.; Pozar, M. *Fuel Economy Benefit of Cylinder Deactivation-Sensitivity to Vehicle Application and Operating Constraints*; SAE Technical Paper 2001-01-3591; SAE International: Warrendale, PA, USA, 2001.
11. Muhamad Said, M.; Latiff, Z.; Zainal Abidin, S.; Zahari, I. Investigation of Intake Valve Strategy on the Cylinder Deactivation Engine. *Appl. Mech. Mater.* **2016**, *819*, 459–465. [\[CrossRef\]](#)
12. Middendorf, H.; Theobald, J.; Lang, L.; Hartel, K. The 1.4-l TSI Gasoline Engine with Cylinder Deactivation. *MTZ Worldw.* **2012**, *73*, 4–9. [\[CrossRef\]](#)
13. Brinklow, G.; Herreros, J.M.; Rezaei, S.Z.; Omid, D.; Millington, P.; Kolpin, A. Impact of Cylinder Deactivation Strategies on Three-way Catalyst Performance in High Efficiency Low Emissions Engines. *Chem. Eng. J. Adv.* **2023**, *14*, 4–9. [\[CrossRef\]](#)
14. Turnbull, R.; Dolatabadi, N.; Rahmani, R.; Rahnejat, H. Energy loss and emissions of engine compression rings with cylinder deactivation. *Proc. Inst. Mech. Eng. Part D J. Automob. Eng.* **2021**, *235*, 1930–1943. [\[CrossRef\]](#)
15. Mohammadpour, M.; Rahmani, R.; Rahnejat, H. Effect of cylinder deactivation on the tribo-dynamics and acoustic emission of overlay big end bearings. *Proc. Inst. Mech. Eng. Part K J. Multi-Body Dyn.* **2014**, *228*, 138–151. [\[CrossRef\]](#)
16. Ma, Z. *Oil Transport Analysis of a Cylinder Deactivation Engine*; SAE Technical Paper 2010-01-1098; SAE International: Warrendale, PA, USA, 2010. [\[CrossRef\]](#)
17. Baykara, C.; Akin Kutlar, O.; Dogru, B.; Arslan, H. Skip cycle method with a valve-control mechanism for spark ignition engines. *Energy Convers. Manag.* **2017**, *146*, 134–146. [\[CrossRef\]](#)
18. Vijayakumar, R.; Akehurst, S.; Liu, Z.; Reyes-Belmonte, M.A.; Brace, C.J.; Liu, D.; Copeland, C. Design and testing a bespoke cylinder head pulsating flow generator for a turbocharger gas stand. *Energy* **2019**, *189*, 116291. [\[CrossRef\]](#)
19. Bech, A.; Shayler, P.J.; McGhee, M. The Effects of Cylinder Deactivation on the Thermal Behaviour and Performance of a Three Cylinder Spark Ignition Engine. *SAE Int. J. Engines* **2016**, *9*, 1999–2009. [\[CrossRef\]](#)
20. Faust, H.; Scheidt, M. Potentials and Constraints of Cylinder Deactivation in the Powertrain. *MTZ Worldw.* **2016**, *77*, 72–77. [\[CrossRef\]](#)
21. Ess, J.V.; Wolk, B.; Fuschetto, J.; Wang, R.; Younkins, M. Method to Compensate Fueling for Individual Firing Events in a Four-Cylinder Engine Operated with Dynamic Skip Fire. *SAE Int. J. Engines* **2018**, *11*, 977–991. [\[CrossRef\]](#)
22. Baratta, M.; Misul, D.; Xu, J. Development and application of a method for characterizing mixture formation in a port-injection natural gas engine. *Energy Convers. Manag.* **2021**, *227*, 113595. [\[CrossRef\]](#)

23. Hoffmann, H.; Loch, A.; Widmann, R.; Kreusen, G.; Meehsen, D.; Rebbert, M. Cylinder Deactivation for Valve Trains with Roller Finger Follower. *MTZ Worldw.* **2009**, *70*, 26–30. [[CrossRef](#)]
24. Maehara, H.; Kitawaki, S.; Abe, T.; Saito, S.; Tsukui, T. *Development of Variable Cylinder Management System for Large Motorcycles—An Effective Way of Reducing Output Change at Switching of the Number of Working Cylinders*; SAE Technical Paper 2010-32-0117; SAE International: Warrendale, PA, USA, 2010. [[CrossRef](#)]
25. Ihlemann, A.; Nitz, N. Cylinder Deactivation a Technology with a Future or a Niche Application? Schaeffler Symposium. 2014. Available online: <https://api.semanticscholar.org/CorpusID:204860287> (accessed on 19 December 2023).
26. Kreuter, P.; Heuser, P.; Reinicke-Murmann, J.; Erz, R.; Stein, P.; Peter, U. Meta-CVD system: An electro-mechanical cylinder and valve deactivation system. *SAE Trans.* **2001**, *110*, 107–117.
27. Flierl, R.; Lauer, F. Mechanically Fully Variable Valvetrain and Cylinder Deactivation. *MTZ Worldw.* **2013**, *74*, 50–57. [[CrossRef](#)]
28. Millo, F.; Mirzaeian, M.; Luisi, S.; Doria, V.; Stroppiana, A. Engine displacement modularity for enhancing automotive s.i. engines efficiency at part load. *Fuel* **2016**, *180*, 645–652. [[CrossRef](#)]
29. Di Maio, D.; Stramaccioni, E.; Misul, D.A.; Napolitano, P.; Beatrice, C. A Multiphysics Co-Simulation Framework of a Gas Engine and Three-Way Catalyst toward a Complete Vehicle Design Model. *Machines* **2022**, *10*, 852. [[CrossRef](#)]
30. Duan, X.; Liu, Y.; Liu, J.; Lai, M.C.; Jansons, M.; Guo, G.; Zhang, S.; Tang, Q. Experimental and numerical investigation of the effects of low-pressure, high-pressure and internal EGR configurations on the performance, combustion and emission characteristics in a hydrogen-enriched heavy-duty lean-burn natural gas SI engine. *Energy Convers. Manag.* **2019**, *195*, 1319–1333. [[CrossRef](#)]
31. Sun, X.; Liu, H.; Duan, X.; Guo, H.; Li, Y.; Qiao, J.; Liu, Q.; Liu, J. Effect of hydrogen enrichment on the flame propagation, emissions formation and energy balance of the natural gas spark ignition engine. *Fuel* **2022**, *307*, 121843. [[CrossRef](#)]

**Disclaimer/Publisher’s Note:** The statements, opinions and data contained in all publications are solely those of the individual author(s) and contributor(s) and not of MDPI and/or the editor(s). MDPI and/or the editor(s) disclaim responsibility for any injury to people or property resulting from any ideas, methods, instructions or products referred to in the content.